Desalination and Water Treatment
www.deswater.com

doi: 10.5004/dwt.2023.30071

313 (2023) 142–151
November

Adsorption performance of oxytetracycline by different modified hydroxyapatite nanoclusters

Jing-qian Xu[a,†], Juan Tian[b,†], Meng-ting Guo[a,†], Wen-bin Li[a,c,*], Bixia Wang[a,*], Hong-yan Deng[a], Feng Shi[c]

[a]*College of Environmental Science and Engineering, China West Normal University, Nanchong Sichuan 637009, China, emails: lwb062@163.com (W.-b. Li), wangbixia@cwnu.edu.cn (B.-x. Wang), 906893676@qq.com (J.-q. Xu), 897036949@qq.com (M.-t. Guo), dhongyan119@163.com (H.-y. Deng)*
[b]*Sichuan Chuanqian Expressway Co., Ltd., Gulin 646500, China, email: 1198234680@qq.com (J. Tian)*
[c]*Key Laboratory of Nanchong City of Ecological Environment Protection and Pollution Prevention in Jialing River Basin, Nanchong, Sichuan 637009, Republic of China, email: 371026250@qq.com (F. Shi)*

Received 7 August 2023; Accepted 3 October 2023

ABSTRACT

To investigate the adsorption performance of different modified hydroxyapatite nanoclusters (nHAs) for oxytetracycline (OTC), amphoteric modification of nHA with 50% and 100% dodecyl dimethyl betaine (BS) was performed to obtain BS-modified nHA (50BS-nHA and 100BS-nHA). Grafting modification of BS-nHA with thiourea–citral (TC) and thiourea–vanillin (TV) was also conducted to acquire TC- and TV-modified BS-nHA (TC-BS-nHA and TV-BS-nHA), respectively. The microscopic morphology of the tested materials was studied by scanning electron microscopy (SEM), Fourier-transform infrared spectroscopy (FTIR), and specific surface area (S_{BET}) detection. Batch method was used to investigate the adsorption characteristic of OTC on the tested materials, and the effects of pH, temperature, and ionic strength on OTC adsorption were compared. Results were as follows: (1) After amphoteric and grafting modification, the pH, cation exchange capacity (CEC), and S_{BET} of nHA decreased, whereas the total organic carbon (TOC) content increased. SEM and FTIR showed that TC and TV were successfully linked to BS-nHA. (2) The isothermal adsorption curves of each test material for OTC were in accordance with the Langmuir model. The maximum adsorption amount (q_m) of OTC ranged from 87.85 to 168.85 mmol/kg, and was in the order of TC-BS-nHA > TV-BS-nHA > BS-nHA > nHA. (3) The OTC adsorption of the test materials was negatively correlated with pH and ionic strength and positively correlated with temperature, and the optimum adsorption conditions were 30°C, pH = 5, and ionic strength of 0.01 mol/L. (4) The results of thermodynamic analysis indicated that the adsorption of OTC was a spontaneous, endothermic, and entropy-increasing reaction. The adsorption of OTC by each tested material conformed to the pseudo-second-order kinetic equation. TOC was the key to determining the adsorption capacity of each test material to OTC.

Keywords: Hydroxyapatite nanocluster; Dodecyl dimethyl betaine; Grafting modification; Oxytetracycline adsorption

1. Introduction

With the progress of urbanization in recent years, the urban population has been increasing, leading to serious pollution of urban rivers and a greater impact on the ecological environment of the cities and their surrounding areas. Therefore, our focus should be shifted to the treatment and

* Corresponding authors.
† These authors have contributed equally to this work and share first authorship.

remediation of water pollution in urban rivers [1]. Antibiotics have the role of preventing diseases and promoting growth, and China is the world's largest producer and consumer of antibiotics; only 15% can be absorbed by the human body and animals, and the remaining 85% is excreted from the body into the environment through metabolism [2]. Given that antibiotics are difficult to biodegrade, their accumulation in the environment will bring serious risks to environmental safety [3]; hence, investigating the adsorption and blocking of antibiotics in water treatment is important for human health and ecosystem safety. Antibiotic removal techniques in water bodies include adsorption [4], photodegradation [5,6] biodegradation [7], and electrochemical degradation [8]. Among them, adsorption is a cheap, convenient, and efficient treatment and purification technology. Yu et al. [9] used a magnetic graphene oxide sponge to adsorb tetracycline with an adsorption capacity of up to 473 mg/g. Similarly, the adsorption of nitroimidazole antibiotics using buckwheat bark biochar was found to increase with temperature, eventually reaching 100%. Ahmed et al. utilized lignocellulosic biochar to adsorb ciprofloxacin and norfloxacin with maximum removal rates of 96.12% and 98.13%, respectively [10]. Moreover, the adsorption of sulfamethoxazole, ciprofloxacin, and trimethoprim in water was explored using composite magnetic nanogel spheres, and the maximum adsorption amounts reached 47.19, 59.65, and 96.47 mg/g, respectively [11]. Existing adsorbent materials have achieved good results in the adsorption of antibiotics, but further studies have revealed that physicochemical-modified materials are more effective in removing pollutants. Qin et al. [12] used modified biochar to effectively adsorb sulfonamides from water and found that the optimal pH and temperature were 4°C and 35°C, respectively. Modified natural fiber materials were adopted to adsorb three tetracycline antibiotics from wastewater, and the removal rates of hygromycin, tetracycline, and doxycycline reached 67.27%, 79.08%, and 87.40%, respectively [13]. A polydopamine-modified salecan hydrogel was prepared to enhance the antibiotic adsorption capacity, and the frontal maximum adsorption coefficients for chlorhexidine acetate, minocycline, and erythromycin were 134.85, 134.65, and 82.24 mg/g, respectively [14]. A hexagonal boron nitride-modified material was used to remove ofloxacin up to 99.74%, and its adsorption capacity reached 305.32 mg/g [15].

Hydroxyapatite ($Ca_{10}(PO_4)_6(OH)_2$, HA) is a compound similar to bioapatite. Given its high adsorption capacity and low water solubility, HA is a good adsorbent for heavy metals, dyes, and other pollutants in wastewater [16]. The maximum adsorption capacity of HA for oxytetracycline (OTC) was up to 139.38 mmol/kg, with optimum pH = 8, and equilibrium was reached within 120 min [17]. The adsorption behavior of OTC on HA was correlated with pH, contact time, adsorbent dose, and OTC concentration, and the removal rate of OTC could reach 97.58% [18]. Studies showed that HA nanoclusters (nHAs) are biomaterials with highly interconnected porous structures and a larger specific surface area (S_{BET}) [19]. If nHA was further modified with different modifiers, the adsorption capacity of nHA could be greatly enhanced. However, reports on the adsorption of OTC on modified nHA are few to date. In this work, dodecyl dimethyl betaine (BS) was used to modify nHA for obtaining BS-modified nHA (BS-nHA). Then, grafting modification of BS-nHA was implemented. The microscopic morphology of the tested materials was studied by scanning electron microscopy (SEM), Fourier-transform infrared spectroscopy (FTIR), and S_{BET} detection. Batch method was used to investigate the adsorption characteristic of OTC on the tested materials, and the effects of pH, temperature, and ionic strength on OTC adsorption were compared. The results of this study will provide a basis for the theory and practice of nHA remediation of OTC pollution in water environments.

2. Materials and methods

2.1. Materials

2.1.1. Experimental surface modifier

BS (purchased from Tianjin Xingguang Auxiliary Factory, analytic reagent) was used as an amphoteric modifier. Thiourea (T, analytic reagent), citral (C, analytic reagent), and vanillin (V, analytic reagent), purchased from Chengdu Cologne Chemical Co., Ltd., were used as the grafting modifiers. The molecular formula of the three modifiers is shown in Fig. 1.

2.1.2. Preparation of nHA

The main raw materials were calcium nitrate tetrahydrate ($Ca(NO_3)_2$-$4H_2O$), disodium hydrogen phosphate dodecahydrate (Na_2HPO_4-$12H_2O$), and urea (CON_2H_4), which were purchased from Chengdu Kelong Chemical Reagent Factory. The template molecule was cyclohexane-1,2,3,4,5,6-hexacarboxylic acid (H_6E) of analytical purity, purchased from Tokyo Kasei Kogyo Co., Ltd. H_6E (5 mmol/L) was added to 0.1 mol/L $Ca(NO_3)_2$-$4H_2O$ solution, then an appropriate amount of Na_2HPO_4-$12H_2O$ was added again, keeping the calcium to phosphorus ratio at 1.67:1. Afterward, 0.56 mol/L CON_2H_4 and dilute nitric acid were added to adjust the pH to 2.5. The solution was transferred to a reaction vessel and reacted at 150°C for 5 h. It was washed and dried to obtain nHA.

2.1.3. Preparation of BS-nHA

A wet process was adopted to prepare BS-nHA [20]. In this process, 100 g of nHA was slowly added to 1.0 L of dH_2O, and different ratios (50% and 100%) of BS, which were calculated in accordance with the cation exchange capacity (CEC) of nHA, were added again. After stirring at 40°C for 3 h, the samples were separated, washed with dH_2O thrice, dried at 60°C for 12 h, and passed through a 60-mesh sieve. Next, 50%BS- and 100%BS-modified nHA were prepared

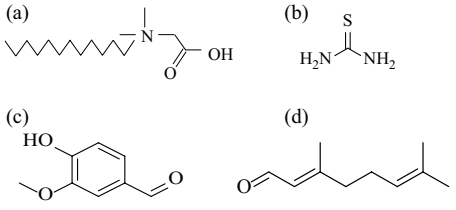

Fig. 1. Molecular structural formula of BS (a), T (b), C (c), and V (d).

and recorded as 50BS-nHA and 100BS-nHA, respectively. The BS weight for a certain weight of nHA can be obtained by using Eq. (1).

$$W = \frac{m \times \mathrm{CEC} \times M \times 10^{-6} \times R}{b} \quad (1)$$

where W (g) refers to the weight of BS, m (g) refers the weight of the nHA that will be modified, CEC (mmol/kg) represents the CEC of nHA, M (g/mol) is the molecular mass of BS, R stands for the modified proportion of BS, and b specifies the product content of BS (mass fraction).

2.1.4. Grafting modification of BS-nHA

50BS-nHA and 100BS-nHA were modified with thiourea–citral (TC) and thiourea–vanillin (TV) through grafting to obtain TC- and TV-modified 50BS-nHA and 100BS-nHA, respectively. The four treatments were expressed as TC-50BS-nHA, TC-100BS-nHA, TV-50BS-nHA, and TV-100BS-nHA. The dosages of TC and TC were calculated in accordance with the wet method.

2.1.5. Preparation of OTC pollutant

The test contaminant OTC was purchased from Sigma, USA, with a purity of 99.9%. As shown in Fig. 2 the hygromycin molecule has three pKa (pK_1 = 3.57, pK_2 = 7.49, pK_3 = 9.44) [21]. At pH < 5.5, OTC is mainly present as cations and amphoteric ions, at 5.5 < pH < 8.7, it is mainly present as amphoteric ions and amidated anions, and at pH > 8.7, amidated and divalent anions are predominant [22].

2.2. Experimental design

2.2.1. Microscopic morphology of the tested materials

The basic physicochemical properties, such as pH, CEC, and total organic carbon (TOC) content of the tested materials were determined. The microscopic morphology of the tested materials was studied by using SEM, FTIR, and S_{BET} detection.

2.2.2. Adsorption isotherm experiment

The concentrations of OTC were set to ten concentration gradients of 0, 0.3, 0.6, 1.2, 3, 6, 12, 18, 24, and 30 mg/L. The temperature was set to 20°C, the pH of the solution was set to 5, and the ionic strength was set to 0.1 mol/L of NaCl.

2.2.3. Influencing factor experiment

Temperature is set at 10°C, 20°C and 30°C (pH value of the solution: 5; ionic strength: 0.1 mol/L). pH values are set at 3, 5, and 7 (initial solution temperature: 20°C; ionic strength: 0.1 mol/L). Ionic strength was set at 0.01, 0.1, and 0.2 mol/L (pH value of the solution: 5; initial solution temperature: 20°C).

2.2.4. Adsorption kinetics of OTC

The adsorption time was set as 5, 10, 30, 60, 120, 180, 240, 300, 360, 480, and 720 min. The temperature was set as 20°C, the pH value of the solution was set as 5, and the ionic strength was set as 0.1 mol/L of NaCl.

2.3. Experimental methods

S_{BET} were analyzed using a multipoint BET method through the Gold APP V-Sorb2800P analyzer (Ultrametrics, Beijing, China). SEM was performed using the Japanese Hitachi S-4800 scanning electron microscope. FTIR analysis was performed on the Nicolet iS50 type Fourier transform infrared spectrometer (ThermoFisher, Massachusetts, USA).

The batch equilibrium method was used for OTC adsorption. A total of 0.1000 g of the sample was weighed in nine 50-mL plastic centrifuge tubes to which 20 mL of OTC solutions with different concentration gradients were respectively added. The samples were oscillated at 20°C and 200 rpm for 12 h at constant temperature and centrifuged at 4,800 rpm for 10 min. The concentration of the OTC in the supernatant was determined, and the equilibrium adsorption amount was calculated by the subtraction method. All the above measurements were substituted into the standard solution for analytical quality control.

2.4. Data processing

2.4.1. Calculation of equilibrium adsorption capacity

Equilibrium adsorption capacity was calculated according to Eq. (2).

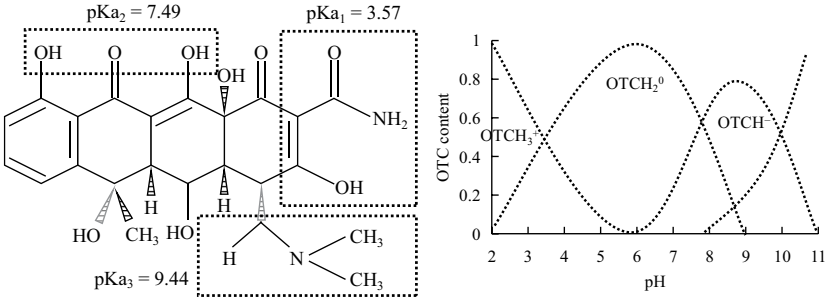

Fig. 2. Structure and pH-dependent speciation of OTC.

$$q_e = \frac{V\left(C_0 - C_e\right)}{m} \tag{2}$$

where C_0 and C_e are the initial concentration and equilibrium concentration of OTC in solution, respectively (mmol/L). V refers the volume of OTC solution added (mL). m is the mass of the tested sample (g). q indicates the equilibrium adsorption capacity of OTC on the tested sample.

2.4.2. Fitting of adsorption isotherms

The Langmuir and Henry model were used to fit the adsorption isotherm of OTC, as shown in Eqs. (3) and (4).

$$q_e = \frac{q_m b C_e}{1 + bC_e} \tag{3}$$

$$q_e = KC_e \tag{4}$$

where q_m is the maximum adsorption amount of OTC for the tested sample, mmol/kg; b is the apparent equilibrium constant of OTC adsorption on the tested sample for the measurement of adsorption affinity. K represents the distribution coefficient of OTC in solid phase adsorbent and solvent, and also represents the OTC binding capacity of the tested sample to a certain extent.

2.4.3. Fitting of adsorption kinetics model

The pseudo-first-order and pseudo-second-order kinetics equation models were used to simulate the adsorption process of OTC on the tested materials [23]. The kinetics equations were defined as Eqs. (5) and (6).

$$\ln\left(q_e - q_t\right) = \ln q_e - k_1 t \tag{5}$$

$$\frac{t}{q_t} = \frac{1}{q_e^2 k_2} + \frac{t}{q_e} \tag{6}$$

where q_t (mmol/kg) is the adsorption capacity corresponding to the adsorbent at time t; k_1 (min^{-1}) and k_2 (mmol/kg·min) are pseudo-first-order and pseudo-second-order reaction rate constants, respectively; t is the adsorption time (min).

2.4.4. Calculation of thermodynamic parameters

Parameter K in the Henry model is equivalent to the apparent adsorption constant of equilibrium constant, and called the apparent thermodynamic parameters [2]; Eqs. (7)–(9):

$$\Delta G = -RT\ln K \tag{7}$$

$$\Delta H = R\left(\frac{T_1 \cdot T_2}{T_2 - T_1}\right) \cdot \ln\left(\frac{K, T_2}{K, T_1}\right) \tag{8}$$

$$\Delta S = \frac{\Delta H - \Delta G}{T} \tag{9}$$

where ΔG is the standard free energy change (kJ/mol), R is a constant (8.3145 J/mol·K), T is the adsorption temperature (T_1 = 283.16 K, T_2 = 303.6 K), ΔH is the enthalpy of adsorption process (kJ/mol), and ΔS is the entropy change of adsorption process (J/mol·K).

CurveExpert 1.4 fitting software was used in isothermal fitting, and Origin 2022 was adopted to improve data plotting. The data were expressed as the means with standard deviation, and different letters indicate significant differences among various amendments. Analysis of variance was performed to determine the effects of amendments, followed by Tukey's honestly significant difference test. Differences of $P < 0.05$ were considered significant.

3. Results and discussion

3.1. Physicochemical and microscopic characteristics of test materials

The basic physical and chemical properties of different modified nHAs are shown in Fig. 3. After the modification of BS, the pH, CEC, and S_{BET} of BS-nHA decreased, whereas the TOC of BS-nHA increased. The changes in physicochemical properties of nHA after 100%BS modification were greater

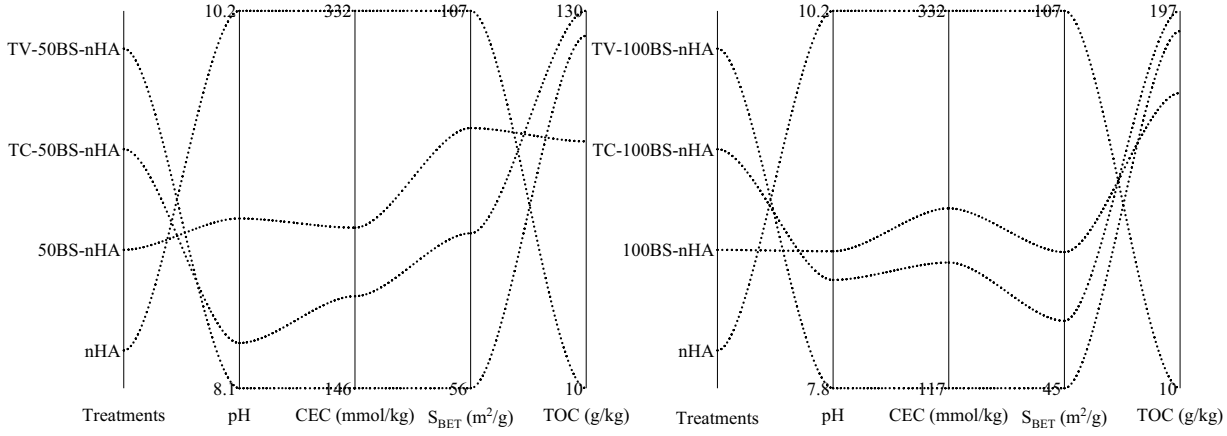

Fig. 3. Physical and chemical properties of test materials.

than those after 50%BS modification. After grafting modification, the pH, CEC, and S_{BET} of different modified nHAs all showed a trend of nHA > BS-nHA > TC-BS-nHA > TV-BS-nHA. The TOC of different modified nHAs exhibited a trend of TC-BS-nHA > TV-BS-nHA > BS-nHA > nHA. S_{BET} of nHA decreased by 32.16%–33.95% after the modification with BS and by 42.33%–43.26% and 55.98%–64.87% after the grafting modification with TC and TV, respectively.

Fig. 4a shows the SEM images of nHA before and after modification. From the image, nHA had a cluster shape with obvious pore structure. When it was modified with BS, the cluster shape of BS-nHA was reduced. After the grafting medication with TC and TV, the original pores of nHA were filled and formed a wall skin-like structure. Fig. 4b presents the FTIR spectra of different modified nHAs. With the modification using BS, TC, and TV, the structural groups in the tested materials did not change the characteristic peak. The absorption peaks with wave numbers around 3,400 cm^{-1} were O–H or N–H stretching vibration absorption peaks, and they overlapped to produce broadened absorption peaks [24]. The vibrational wave numbers near 1,600 cm^{-1} were mainly C=C stretching vibration characteristic peaks, and BS modification made their absorption intensity larger, which proved that BS was successfully attached to nHA. The peaks near 1,400 and 1,048 cm^{-1} were C=O and C=S characteristic peaks, respectively [22], which confirmed that TV and TC were successfully grafted onto BS-nHA.

3.2. Isothermal adsorption characteristics of OTC

The adsorption isotherms of OTC on the modified nHAs under the condition of 20°C, pH = 5, and ionic strength of 0.1 mol/L are shown in Fig. 5a and b. The OTC adsorption capacity of different modified nHAs increased with the increase in equilibrium concentration, showing linear adsorption curves. At the same equilibrium concentration, the OTC adsorption capacity of the modified nHAs was higher than that of unmodified nHA. The Langmuir and Henry models were used to fit the adsorption isotherms of OTC by different modified nHAs (Table 1). The fitting correlation reached a highly significant level ($P < 0.01$), and the fitting effect of the Langmuir model was better than that of Henry model.

The maximum adsorption capacity (q_m) values of OTC on each modified nHA was 87.85–168.85 mmol/kg, ranking in the order of TC-BS-nHA > TV-BS-nHA > BS-nHA > nHA.

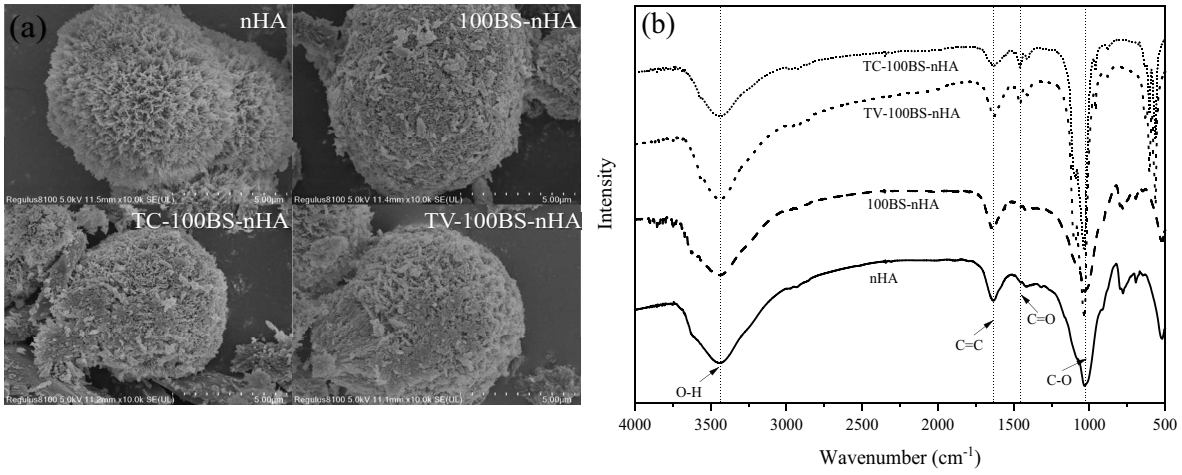

Fig. 4. Scanning electron microscopy (a) and Fourier-transform infrared spectroscopy (b) characteristics of different materials.

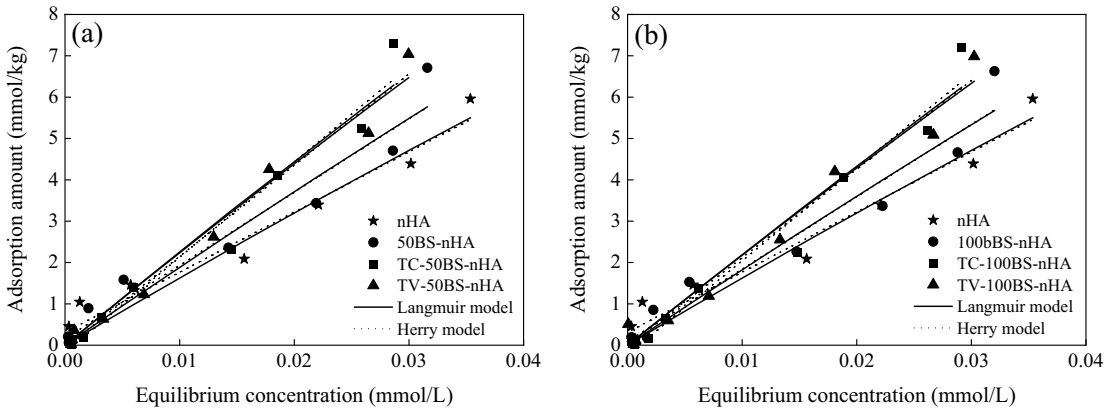

Fig. 5. Isothermal adsorption curve of OTC on test materials.

The q_m values of OTC on 100BS-nHA was higher than that on 50BS-nHA. Compared with that on raw nHA, the adsorption amount of OTC on modified nHA was increased by 35.89%–46.42% (BS-nHA) and 39.51%–92.20% (grafting-modified BS-nHA). The distribution coefficient (K) of OTC adsorption presented the same trend as q_m. The adsorption affinity (b) of the Langmuir model changed within 1.32–1.89, indicating that modified nHAs had low adsorption affinity to OTC. The modification of nHA enriched the functional group of nHA, thus promoting the reaction between antibiotics and nHA materials and facilitating the adsorption of antibiotics [24]. The above results are similar to those of modification of clay, biochar, and other materials [25].

3.3. Effect of pH and ionic strength on OTC adsorption

Under the conditions of 30 mg/L of OTC, 20°C, ionic strength of 0.1 mol/L, and pH range of 3–7, the OTC adsorption amount of each modified nHA first increased and then decreased with the increase in pH, reaching the maximum value at pH = 5, as shown in Fig. 6. When pH changed from 3 to 5, the adsorption of OTC increased by 25.34%–44.73%. OTC is positively charged at pH values below 3.30, can exist as positively or negatively charged species between pH 3.30 and 7.69, and is predominantly in anionic form at pH above 9.50 [26]. Under the conditions of pH = 5, OTC exists mainly as amphoteric ions, which are more likely to interact with the modified nHA [27], so the adsorption of the modified nHAs is better. As the pH increased, OTC started to take on the same negative charge as the surface of the modified nHAs and electrostatic repulsion occurred, which affected the OTC adsorption.

Fig. 7 depicts the effect of ionic strength on the adsorption of OTC by the modified nHAs. The adsorption amounts of OTC exhibited a decreasing trend as the ionic strength increased from 0.01 to 0.2 mol/L, with the peak adsorption observed at an ionic strength of 0.01 mol/L, and the adsorption amount of OTC decreased by 24.04%–28.97%. This observation could be attributed to the influence of ionic strength on the hydrophobic properties of antibiotic molecules. When the concentration of electrolyte cations was high, the adsorption sites on the surface of the modified nHAs were occupied by these cations, which formed an ion exchange competition with OTC for adsorption, resulting in a decrease in the amount of OTC adsorbed [28].

Table 1
Langmuir fitting parameters of OTC adsorption

Test material	Langmuir model			Herry model	
	r	q_m (mmol/kg)	b	r	K
nHA	0.9751**	87.85	1.89	0.9609**	145.46
50BS-nHA	0.9724**	119.38	1.61	0.9430**	177.30
TC-50BS-nHA	0.9801**	166.48	1.38	0.9608**	230.45
TV-50BS-nHA	0.9898**	122.56	1.86	0.9787**	220.54
100BS-nHA	0.9733**	128.63	1.44	0.9434**	174.80
TC-100BS-nHA	0.9797**	168.85	1.32	0.9618**	226.27
TV-100BS-nHA	0.9868**	136.17	1.63	0.9721**	214.02

Note: ** indicates significant correlation at the P = 0.01 level.

3.4. Effect of temperature on OTC adsorption

Under the conditions of pH = 5 and ionic strength of 0.1 mol/L, the influence of temperature on the adsorption of OTC by different modified nHAs is shown in Fig. 8. As the temperature increased from 10°C to 30°C, the adsorption amount of OTC by the modified nHAs increased, indicating a positive temperature effect [11]. The adsorption amounts of OTC by the modified nHAs increased by 14.27%–47.05% as the temperature changed from 10°C to 30°C. With the increase in temperature, the rate of diffusion movement of OTC molecules in the solution increased, and the contact rate with the surface of the modified nHAs was accelerated, thereby increasing the heat absorption reaction between OTC and the modified nHAs. Consequently, the adsorption of OTC increased with the increase in temperature.

Table 2 shows the thermodynamic parameters of the adsorption of OTC on the modified nHAs. At 10°C and 30°C,

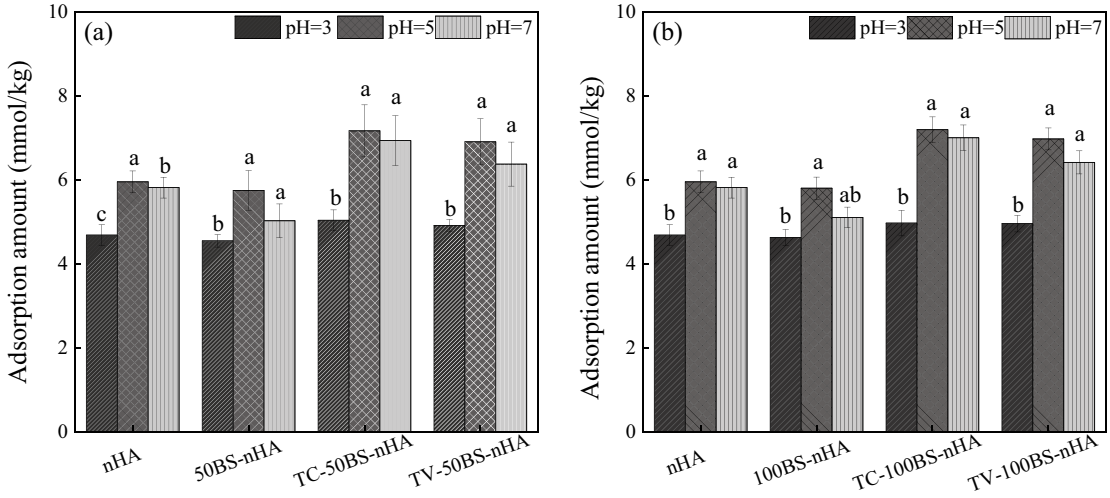

Fig. 6. Effect of pH on the adsorption of OTC by test materials.

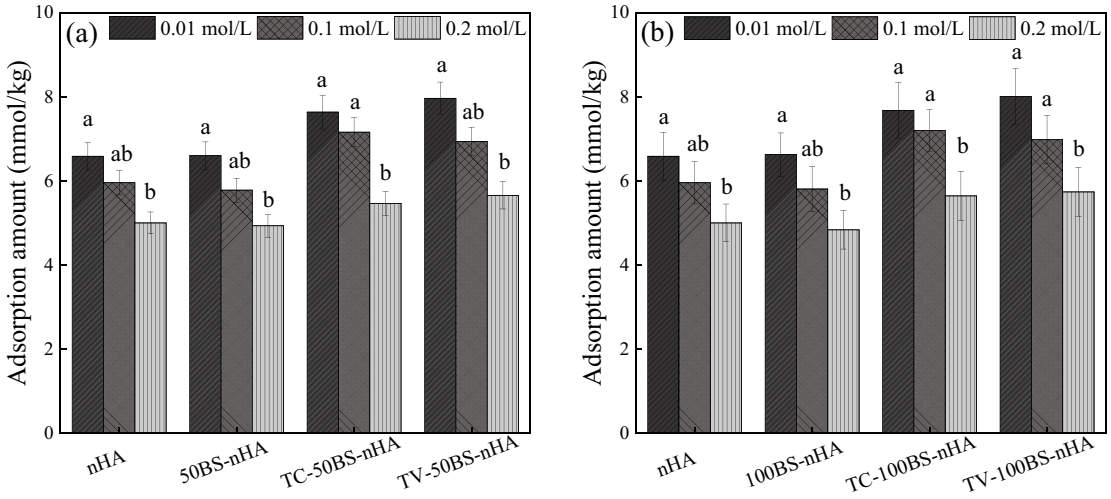

Fig. 7. Effect of ionic strength on the adsorption of OTC by test materials.

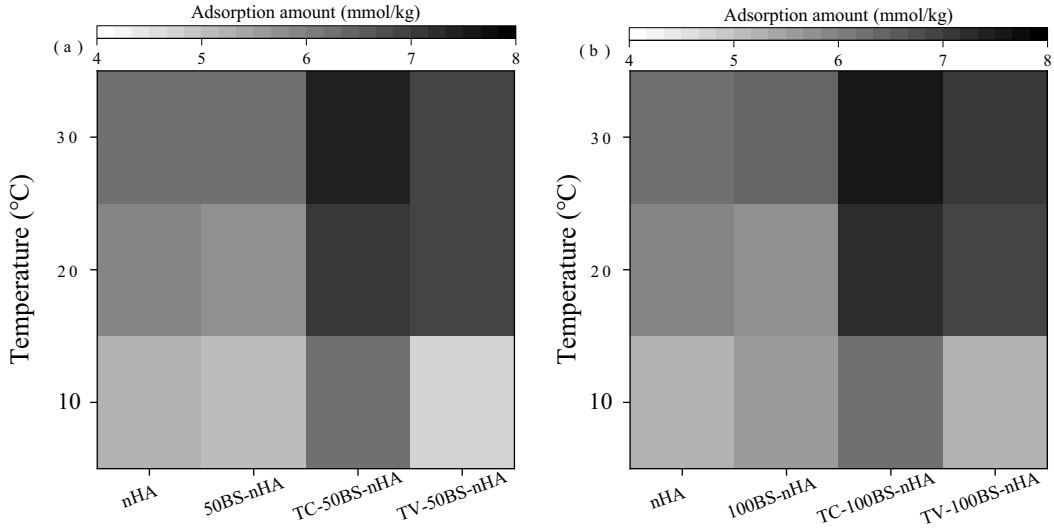

Fig. 8. Effect of temperatures on OTC adsorption by test materials.

Table 2
Thermodynamic parameters of OTC adsorption by test materials

Test material	Δ*G* (kJ/mol)		Δ*H* (kJ/mol)	Δ*S* (J/mol·K)
	10°C	30°C		
nHA	–17.45	–19.01	3.17	72.81
50BS-nHA	–17.11	–18.60	3.08	71.32
TC-50BS-nHA	–16.70	–18.21	3.20	70.27
TV-50BS-nHA	–16.82	–18.97	4.44	75.09
100BS-nHA	–17.01	–18.33	2.75	69.80
TC-100BS-nHA	–16.60	–18.10	3.20	69.91
TV-100BS-nHA	–16.75	–18.64	3.94	73.06

the Gibbs free energy variation (Δ*G*) of OTC adsorption on each modified nHA was less than 0. That is, the adsorption process of OTC was spontaneous, and the spontaneity at 30°C was stronger than at 10°C under the same material. The enthalpy change (Δ*H*) of the modified nHAs was greater than 0, indicating that the adsorption was an endothermic reaction. An increase in temperature could increase the thermal process of OTC and promote the chemisorption process. The entropy change (Δ*S*) of the modified nHAs was greater than 0, implying that the adsorption belonged to entropy-increasing reaction. Hence, the randomness of OTC at the solid–liquid interface increased during the adsorption process [29].

3.5. Kinetic characteristics of OTC adsorption on test materials

The adsorption kinetic curves of OTC on different modified nHAs are shown in Fig. 9. OTC reached adsorption equilibrium at approximately 240 min. The adsorption of OTC on the modified nHAs was simulated using pseudo-first-order and pseudo-second-order kinetic equation models. The fitting parameters of the adsorption kinetics are shown in

Table 3. The adsorption kinetics of all antibiotics conformed to the pseudo-second-order kinetic equation. The R^2 values of the pseudo-second-order kinetic equation for OTC adsorption were higher than those of the pseudo-first-order kinetic equation. Therefore, the pseudo-second-order kinetic equation model accurately described the adsorption kinetics. The results showed that the adsorption of OTC by the modified nHAs was primarily driven by chemisorption, consistent with the observed temperature effect [30].

3.6. Influencing factors and mechanisms of OTC adsorption

q_m and K of OTC adsorption were linearly fitted with the physicochemical properties of the test materials, and the fitting results are shown in Table 4. q_m of the test materials was negatively correlated with pH, CEC, and S_{BET}, whereas q_m significantly positively correlated with TOC. K of the test materials was significantly negatively correlated with pH, CEC, and S_{BET}, whereas q_m significantly positively correlated

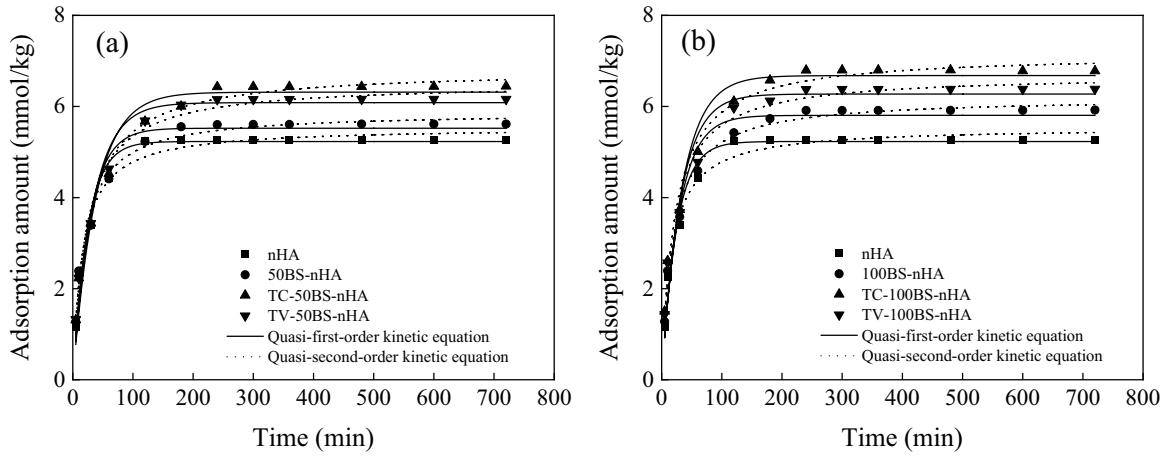

Fig. 9. Adsorption kinetics of OTC on test materials.

Table 3
Kinetic parameters of OTC adsorption by test materials

Treatments	Pseudo-first-order kinetic equation			Pseudo-second-order kinetic equation		
	q_e (mol/kg)	k_1 (min^{-1})	R^2	q_e (mol/kg)	k_2 (kg/mol·min)	R^2
nHA	5.23	0.04	0.9737**	5.55	0.11	0.9851**
50BS-nHA	5.50	0.04	0.9516**	5.88	0.009	0.9876**
TC-50BS-nHA	6.13	0.03	0.9601**	6.81	0.005	0.9882**
TV-50BS-nHA	6.11	0.03	0.9700**	6.52	0.006	0.9885**
100BS-nHA	5.80	0.03	0.9737**	6.19	0.008	0.9919**
TC-100BS-nHA	6.67	0.03	0.9598**	7.16	0.006	0.9847**
TV-100BS-nHA	6.27	0.03	0.9520**	6.70	0.007	0.9855**

Table 4
Effect of physicochemical properties of test materials on q_m and k

Adsorption parameters	Physicochemical properties	Regression equation	r	S
q_m	pH	pH = –0.0183q_m + 11.12	0.6637	0.64
	CEC	CEC = –1.424q_m + 392.10	0.5831	61.30
	S_{BET}	S_{BET} = –0.4555q_m + 131.88	0.5796	19.78
	TOC	TOC = 1.797q_m – 111.39	0.7891*	43.21
K	pH	pH = –0.0204K + 12.74	0.8531**	0.44
	CEC	CEC = –1.745K + 549.22	0.8241*	42.75
	S_{BET}	S_{BET} = –0.5099K + 172.54	0.7483*	16.10
	TOC	TOC = 1.457K – 161.58	0.7374*	47.51

Note: ** and * indicate a significant correlation at P = 0.01 and p = 0.05 levels, respectively.

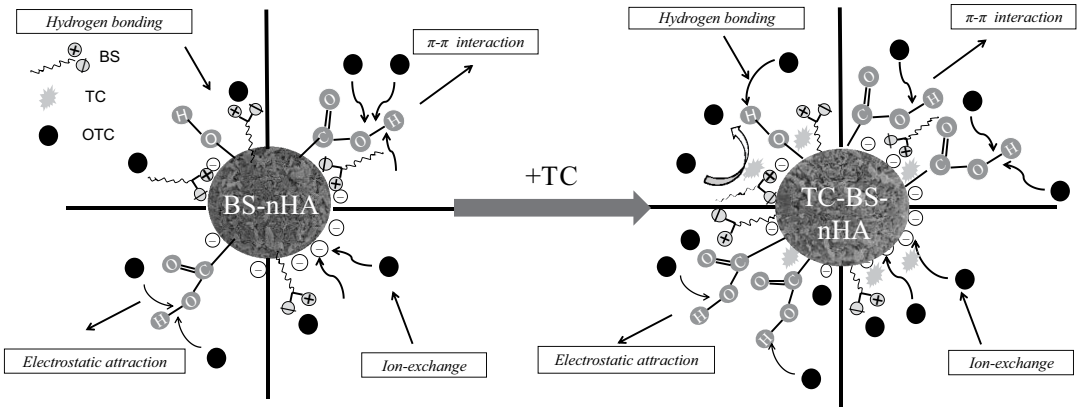

Fig. 10. OTC adsorption mechanism diagram of test materials.

with TOC. Hence, TOC was the key to determining the adsorption effect of OTC by the tested materials. The TOC of the test materials could provide a large number of functional groups and adsorption sites for OTC, promoting the OTC adsorption [31].

Fig. 10 shows the OTC adsorption mechanism diagram of the test materials. After modification with BS, the $-N^+$ on the hydrophilic group of BS bound to the negative charge on nHA surface, and the hydrophobic carbon chain on BS extended outward to form an organic phase on the surface [32]. The carboxyl group contained on BS produced π–π interactions with OTC, and the functional group O–H on the test material was hydrogen bonded with OTC. In addition, the modified material exhibited ion exchange and electrostatic attraction with OTC to improve the adsorption capacity. After grafting modification, the addition of nitrogen- and oxygen-containing functional groups to OTC increased the acidity of nHA and enhanced its CEC and electrostatic attraction.

4. Conclusion

The pH, CEC, and S_{BET} of nHA decreased and the TOC content of nHA increased after amphoteric and grafting modification. SEM and FTIR showed that TC and TV were successfully linked to BS-nHA. q_m of OTC ranged from 87.85 to 168.85 mmol/kg and was in the order of TC-BS-nHA > TV-BS-nHA > BS-nHA > nHA. The OTC adsorption of the modified nHAs was negatively correlated with pH and ionic strength and positively correlated with temperature, and the optimum adsorption conditions were 30°C, pH = 5, and ionic strength of 0.01 mol/L. The thermodynamic analysis indicated that the adsorption of OTC was a spontaneous, endothermic, and entropy-increasing reaction. OTC adsorption by the modified nHAs was in accordance with the quasi-secondary kinetic equation, and TOC was the key to determining the adsorption capacity of OTC. For practical application, the modified nHAs has economic, ecological, and effective advantages and high application value for pollution remediation.

Acknowledgements

The authors wish to acknowledge and thank the Sichuan Transportation Technology Project (2021-ZL-8), the Fundamental Research Funds of China West Normal University (18B023; 20A022), and the Tianfu Scholar Program of Sichuan Province (2020–17).

Conflict of interests

The authors declare that they have no conflict of interest.

References

[1] W.B. Li, X.Y. Chen, H.Y. Deng, D. Wang, J.C. Jiang, Y.Z. Zeng, L. Kang, Z.F. Meng, Effects of exogenous biochar on tetracycline adsorption by different riverbank soils from Sichuan and Chongqing section of Jialing River, Chin. J. Soil Sci., 51 (2020) 46–54.
[2] Y. Zou, H.Y. Deng, M. Li, Y.H. Zhao, W.B. Li, Enhancing tetracycline adsorption by riverbank soils by application of biochar-based composite materials, Desal. Water Treat., 207 (2020) 332–340.
[3] X.H. Liu, S.Y. Lu, W. Guo, B.D. Xi, W.L. Wang, Antibiotics in the aquatic environments: a review of lakes, China, Sci. Total Environ., 627 (2018) 1195–1208.
[4] W.A. Khanday, M.J. Ahmed, P.U. Okoye, E.H. Hummadi, B.H. Hameed, Single-step pyrolysis of phosphoric acid-activated chitin for efficient adsorption of cephalexin antibiotic, Bioresour. Technol., 280 (2019) 255–259.
[5] A. Efraim, F. Ferraro, J. Silva-Agredo, R.A. Torres-palma, Degradation of highly consumed fluoroquinolones, penicillins and cephalosporins in distilled water and simulated hospital wastewater by UV_{254} and UV_{254}/persulfate processes, Water Res., 122 (2017) 128–138.
[6] J.X. Zhang, M.L. Xie, H.Y. Zhao, L.R. Zhang, G.F. Wei, G.H. Zhao, Preferential and efficient degradation of phenolic pollutants with cooperative hydrogen-bond interactions in photocatalytic process, Chemosphere, 269 (2021) 129–404.
[7] J.J. Jiang, C.L. Li, M.D. Fang, Emerging organic contaminants in coastal waters: anthropogenic impact, environmental release and ecological risk, Mar. Pollut. Bull., 85 (2014) 357–399.
[8] E.A. Serna-Galvis, K.E. Berrio-Perlaza, R.A. Torres-Palma, Electrochemical treatment of penicillin, cephalosporin, and fluoroquinolone antibiotics via active chlorine: evaluation of antimicrobial activity, toxicity, matrix, and their correlation with the degradation pathways, Environ. Sci. Pollut. Res., 24 (2017) 23771–23782.
[9] B. Yu, Y. Bai, Z. Ming, H. Yang, L. Chen, X. Hu, S. Feng, S.-T. Yang, Adsorption behaviors of tetracycline on magnetic graphene oxide sponge, Mater. Chem. Phys., 198 (2017) 283–290.
[10] M.J. Ahmed, S.K. Theydan, Fluoroquinolones antibiotics adsorption onto microporous activated carbon from

lignocellulosic biomass by microwave pyrolysis, J. Taiwan Inst. Chem. Eng., 45 (2014) 219–226.
[11] W.A. Khanday, B.H. Hameed, Zeolite-hydroxyapatite-activated oil palm ash composite for antibiotic tetracycline adsorption, Fuel, 215 (2018) 499–505.
[12] P.Z. Qin, D.W. Huang, R. Tang, F.Q. Gan, Y. Guan, X.X. Lv, Enhanced adsorption of sulfonamide antibiotics in water by modified biochar derived from bagasse, Open Chem., 17 (2019) 1309–1316.
[13] X. Liu, Y.F. Zhang, P. Luo, Study on the modification of natural fiber materials and their application of antibiotic adsorption, J. Agro-Environ. Sci., 10 (2013) 2061–2065.
[14] R.Y. Geng, J. Wang, Z. Zhang, Q.J. Dong, F.F. Wu, S.S. Chen, T. Su, X.L. Qi, Adsorption of antibiotics by polydopamine-modified salecan hydrogel: performance, kinetics and mechanism studies, Chem. Eng. J., 454 (2023) 140446, doi: 10.1016/j.cej.2022.140446.
[15] Y. Wang, Y. Fang, Y. Gu, K. Guo, Z. Guo, C. Tang, Enhanced adsorption of fluoroquinolone antibiotics on Cu-modified porous boron nitride nanofibers in aqueous solution, J. Mol. Struct., 1255 (2022) 132475, doi: 10.1016/j.molstruc.2022.132475.
[16] P. Gouma, R. Xue, C.P. Goldbeck, P. Perrotta, C. Balázsi, Nano-hydroxyapatite-cellulose acetate composites for growing of bone cells, Mater. Sci. Eng. C, 32 (2012) 607–612.
[17] L. Yuan, M. Yan, Z.Z. Huang, K. He, G.M. Zeng, A.W. Chen, L. Hu, H. Li, M. Peng, T.T. Huang, G.Q. Chen, Influences of pH and metal ions on the interactions of oxytetracycline onto nano-hydroxyapatitle and their co-adsorption behavior in aqueous solution, J. Colloid Interface Sci., 541 (2019) 101–113.
[18] M. Harja, G. Ciobanu, Studies on adsorption of oxytetracycline from aqueous solutions onto hydroxyapatite, Sci. Total Environ., 628–629 (2018) 36–43.
[19] Z.L. Wang, N. Zhang, Y. Wang, P.B. Zhang, Preparation and properties of mesoporous nanohydroxyapatite/levulinic acid composites, J. Compos. Mater., 32 (2015) 1681.
[20] Y.Z. Wang, Z.H. Shan, Preparation and application overview of hydroxyapatite (HAP), J. Leather Sci. Eng., 25 (2015) 34–38.
[21] S. Liu, P. Wu, M. Chen, L. Yu, C. Kang, N. Zhu, Z. Dang, Amphoteric modified vermiculites as adsorbents for enhancing removal of organic pollutants: bisphenol A and tetrabromobisphenol A, Environ. Pollut., 228 (2017) 277–286.
[22] Y.F. Wang, H.Y. Deng, W.B. Li, A. Touqeer, M. Li, J.N. Wu, J.M. Ouyang, Litter extract from *Alternanthera philoxeroides* as an efficient passivator for oxytetracycline stability in riverbank purple soils, Environ. Technol. Innovation, 29 (2023) 103022, doi: 10.1016/j.eti.2023.103022.
[23] S. Chowdhury, P. Saha, Adsorption kinetic modeling of safranin onto rice husk biomatrix using pseudo-first-and pseudo-second-order kinetic models: comparison of linear and non-linear methods, Clean-Soil, Air, Water, 39 (2011) 274–282.
[24] W.B. Li, M.T. Guo, Y.F. Wang, H.Y. Deng, H. Lei, C.T. Yu, Z.F. Liu, Selective adsorption of heavy metal ions by different composite-modified semi-carbonized fibers, Sep. Purif. Technol., 328 (2023) 125022, doi: 10.1016/j.seppur.2023.125022.
[25] N. Cheng, B. Wang, P. Wu, X. Lee, B. Gao, Adsorption of emerging contaminants from water and wastewater by modified biochar: a review, Environ. Pollut., 273 (2021) 116448, doi: 10.1016/j.envpol.2021.116448.
[26] W. Liu, H. Wang, X.J. Chen, D.W. Yang, G.W. Kuang, Z.L. Sun, Progress on degradation of antibiotics in environment, Prog. Vet. Med., 30 (2009) 89–94.
[27] C.A. Andrade, L.A. Zambrano-Intriago, N.S. Oliveira, J.S. Vieira, J.M. Rodríguez-Díaz, Adsorption behavior and mechanism of oxytetracycline on rice husk ash: kinetics, equilibrium, and thermodynamics of the process, Water Air Soil Pollut., 231 (2020) 1–16.
[28] S. Chiarle, M. Ratto, M. Rovatti, Mercury removal from water by ion exchange resins adsorption, Water Res., 34 (2000) 2971–2978.
[29] Z.F. Liu, W.B. Li, Q. Liang, X. Fang, H.Y. Deng, Environmental effects on antibiotic adsorption by Fe/Mn-loaded amphoteric clay, Desal. Water Treat., 265 (2022) 146–156.
[30] H. Wang, H.T. Shen, C. Shen, Y.N. Li, Z.F. Ying, Y.F. Duan, Kinetics and mechanism study of mercury adsorption by activated carbon in wet oxy-fuel conditions, Energy Fuels, 33 (2019) 1344–1353.
[31] R.A. Figueroa, A. Leonard, A. Mackaya, Modeling tetracycline antibiotic sorption to clays, Environ. Sci. Technol., 38 (2004) 476–483.
[32] H.Y. Deng, H.X. He, W.B. Li, T. Abbas, Z.F. Liu, Characterization of amphoteric bentonite-loaded magnetic biochar and its adsorption properties for Cu^{2+} and tetracycline, PeerJ, 10 (2022) 13030–13049.